ESTIMATION OF AERODYNAMIC PARAMETERS FROM FLIGHT DATA OF A HIGH INCIDENCE RESEARCH MODEL

V. Klein
George Washington University-JIAFS
NASA Langley Research Center

and

M. H. Mayo
NASA Langley Research Center
Hampton, Virginia, USA

Abstract

A procedure for the determination of an aerodynamic model structure and aerodynamic parameters is applied to flight data from a high-incidence research model (HIRM) within an angle of attack range of 18 to 40 degrees. The HIRM is a three-surface unpowered model with a swept wing, an all-moving canard and stabilator, and a vertical tail with rudder. The motion of the HIRM was excited first by its release from the helicopter and then by the activation of control surfaces. This paper briefly describes the model, flight and wind tunnel data available, equations of motion and techniques for data analysis. The results presented contain an example of a measured data compatibility and the variation of some important stability derivatives with the angle of attack and canard setting. The derivatives were obtained from various maneuvers and subsets of joined data from several maneuvers by using a stepwise-regression technique. These derivatives agreed, in general, with the results of wind-tunnel measurements. The resulting lateral aerodynamic model equations could predict the motion of the HIRM reasonably well.

Notation

Only the main and the most frequently used symbols are introduced. The other symbols are explained in the body of the paper.

a_x, a_y, a_z	longitudinal, lateral and vertical accelerations, g units
b	wing span, m
$\bar{c}$	mean aerodynamic chord, m
C_a	general aerodynamic force and moment coefficient
$C_{X,Y,Z}$	longitudinal-, lateral- and vertical-force coefficient
$C_{\ell,m,n}$	rolling-, pitching- and yawing-moment coefficient
I_X, I_Y, I_Z	moments of inertia about longitudinal, lateral, and vertical body axes, kg-m^2
I_{XZ}	product of inertia, kg-m^2
m	mass, kg
p,q,r	roll rate, pitch rate and yaw rate, rad/sec or deg/sec
S	wing area, m^2
u,v,w	longitudinal, lateral and vertical airspeed components, m/sec
V	airspeed, m/sec
α	angle of attack, rad or deg
β	angle of sideslip, rad or deg
θ	pitch angle, rad or deg
ϕ	roll angle, rad or deg
$\delta_{d,h,r,c}$	differential tail, symmetric tail, rudder and canard deflections, rad

Stability derivatives are referenced to a system of body axes with the origin at the airplane center of gravity.

$$C_{a_\beta} = \frac{\partial C_a}{\partial \beta}, \qquad C_{a_p} = \frac{\partial C_a}{\partial \frac{pb}{2V}}, \quad (a = Y, \ell, \text{ or } n)$$

$$C_{m_q} = \frac{\partial C_m}{\partial \frac{q\bar{c}}{2V}}$$

I. Introduction

In 1982, the Royal Aircraft Establishment (RAE) in Farnborough, England, initiated a program of research on the flight dynamics of departure using a high-incidence research model (HIRM). The main objective of this program was stated in [1] as "the widening of understanding of the flight dynamics phenomena of control aircraft at high angles of attack. Central to this is the development of mathematical modeling techniques to predict such phenomena at or near departure at low speeds, and to provide data from free-flight and wind-tunnel experiments for this purpose." Both wind-tunnel and free-flight drop tests have been employed in pursuit of that objective.

A correlation of behavior predicted from the wind tunnel derived model and free flight responses near departure conditions were presented in [2]. Under a Memorandum of Agreement between the RAE and NASA in the area of departure prediction, researchers from George Washington University and NASA Langley Research Center have been involved in the analysis of flight data from five drop tests of the HIRM. The purpose of the paper is to present an application of system identification to the analysis of measured data from those drop tests and to determine a mathematical model of HIRM. The paper starts with a brief description of the HIRM and flight data available for the analysis. Then, the RAE wind tunnel experiment is briefly mentioned. The next section covers the airplane equations of motion and the postulated aerodynamic mathematical models. This is followed by a section on the data analysis which includes a compatibility check of measured data using a nonlinear fixed-interval smoother, and aerodynamic model structure determination and parameter estimation based on a stepwise regression. The last major section presents the main results of the study in the form of stability and control derivatives and their variation with the angle of attack and canard setting. Some of the estimated parameters obtained both from individual maneuvers and partitioned data are shown and compared with wind tunnel results. Finally, the mathematical model of the HIRM is verified by a comparison of the measured and predicted time histories of aerodynamic coefficients and response variables.

II. High Incidence Research Model (HIRM)

The HIRM is a three-surface unpowered model with an advanced transonic swept wing, an all-moving canard and stabilator, and an oversized vertical tail with rudder. The wing has no moving control surfaces. Roll control is provided by differential canard and stabilator deflection. The general arrangement of the model is shown in Figure 1. The model is fully instrumented with the transducer signals telemetered to a ground station. A nose boom carrying angle-of-attack and sideslip vanes, and a pitot-static probe have been included. Flight maneuvers are preprogrammed into the system and executed by a timer after the model is released from a carrier helicopter.

The model was flight tested at NASA Dryden Flight Research Facility, Edwards, California. During those tests the model was towed by helicopter to 3,000-4,000 meters above the impact range and released at a speed of approximately 150 km/-hour. At the time of release a timer began a preprogrammed test sequence which activated a series of switches thus positioning the model's flight control surfaces. The duration of the flights varied between 80 and 160 sec. At a predetermined time, or at a given height above ground, three parachutes were deployed to recover the model. The landing was cushioned by low pressure air bags which were deployed from a door beneath the fuselage.

III. Flight Data

The motion of the HIRM was initially excited by the model's release from the helicopter cable and then by the activation of control surfaces. For each test run either doublet in differential tail or canard, or simple rudder pulse were used. In some maneuvers a step deflection of symmetric tail was added. The various trim conditions were established by the canard setting at either 0° or -10° and by the tailplane setting between -14° to -20°. Most of the responses were within the α-range of 20° to 40° though in three maneuvers α reached 60°.

The measured data from five flights with 26 maneuvers were obtained as time histories of control and response variables sampled at 0.012 sec intervals. The two flights with $\delta_c \doteq -10°$ and $\delta_h \doteq -18°$ are designated as HD1 and HD3, the remaining three flights with $\delta_c \doteq 0°$ and $\delta_h \doteq -15°$, as HD2, HD4 and HD6. When appropriate, the measured data were corrected for the e.g. offset and air flow effect. One example of a test run is given in Figure 2. It represents the motion of the model following its release and differential tail doublet of the duration of approximately 3 sec applied at $t \doteq 23$ sec.

In addition to analyzing almost all of the 26 individual maneuvers, the data from each flight were joined together into one set of data. The resulting ensemble was then partitioned into subsets according to the value of α (see [3] explaining the partitioning procedure and its impact on model simplification). For these new subsets of data, the aerodynamic coefficients were modeled mostly on 1° subspaces of the original α-space.

IV. Wind Tunnel Measurements

The program for wind tunnel measurements of the HIRM is outlined in [1]. This program includes static, oscillatory and steady rolling tests using models of various sizes. Results from low-speed static tests of a preliminary model in the RAE (Farnborough) 11 1/2 -by 8-foot and RAE (Bedford) 13-by-9-foot wind tunnels are given in [4]. These tests covered a wide range of α, mostly from 0° to 40°, and sideslip changes between ±6°. During these tests the canard and tailplane were deflected both symmetrically and differentially. The effect of rudder deflection was also measured in combination with the differential canard and tailplane. From these measurements, some of the stability and control derivatives were evaluated. A selection of configurations from [4] was repeated with a 4/9-scale definitive model tested in the RAE (Bedford) 13-by 9-foot tunnel. The unpublished results were mostly obtained with a tunnel speed of 70 m/sec, i.e., at a Reynolds number close to that in free-flight experiment.

The 4/9-scale model was also tested on an oscillatory rig over an α-range of 0° to 85° for rolling and yawing motions at various control settings, and for $0° < \alpha < 60°$ in pitch for three canard settings. The wind speed in the RAE (Bedford) 13-by 9-foot tunnel was 70 m/sec for $\alpha < 25°$, and 40 m/sec for $\alpha > 25°$. The results of these tests are reported in [5]. Steady rolling tests were conducted on both 4/9-scale model and BAe Warton [6], and on the 2/9-scale model at RAE Bedford [7]. The agreement between both tests was very good. However, substantial differences in roll-damping and cross-terms obtained from the steady rolling tests and oscillatory tests within α-range of 20° to 30° were observed.

V. Equations of Motion

The HIRM equations of motion are referred to body axes and they have the form

$$\dot{u} = -qw + rv - g \sin\theta + \frac{\rho V^2 S}{2m} C_X$$

$$\dot{v} = -ru + pw + g \cos\theta \sin\phi + \frac{\rho V^2 S}{2m} C_Y$$

$$\dot{w} = -pv + qu + g \cos\theta \cos\phi + \frac{\rho V^2 S}{2m} C_Z$$

$$\dot{p} = \frac{I_Y - I_Z}{I_X} qr + \frac{I_{XZ}}{I_X}(pq + \dot{r}) + \frac{\rho V^2 S b}{2 I_X} C_\ell \qquad (1)$$

$$\dot{q} = \frac{I_Z - I_X}{I_Y} pr + \frac{I_{XZ}}{I_Y}(r^2 - p^2) + \frac{\rho V^2 S \bar{c}}{2 I_Y} C_m$$

$$\dot{r} = \frac{I_X - I_Y}{I_Z} pq + \frac{I_{XZ}}{I_Z}(\dot{p} - qr) + \frac{\rho V^2 S b}{2 I_Z} C_n$$

$$\dot{\phi} = p + (q \sin\phi + r \cos\phi) \tan\theta$$

$$\dot{\theta} = q \cos\phi - r \sin\phi$$

For individual maneuvers, the aerodynamic coefficients were postulated as functions of response and control variables and their combinations as follows:

1. The longitudinal coefficients C_X, C_Z, and C_m

as functions of α, q, δ_h, α^2, $q\alpha$, α^3, $q\alpha^2$, β^2, $\beta^2\alpha$, p, r, δ_d, δ_r, δ_c

2. The lateral coefficients C_Y, C_ℓ, and C_n as functions of β, p, r, δ_d, δ_r, δ_c, $\beta\alpha$, $p\alpha$, $r\alpha$, $\beta\alpha^2$, $p\alpha^2$, $r\alpha^2$, β^2, p^2, β^3, p^3, $\beta^2\alpha$, $p^2\alpha$, $\beta^3\alpha$, $p^3\alpha$, $p\beta$, α, α^2, α^3

In both cases the functions were approximated by polynomials. The variables in these polynomials represent the increments with respect to their trim values. In the equation for the pitching moment coefficient, the term $\dot{\alpha}$ could not explicitly be included because of identifiability problems which occur due to high correlation between $\dot{\alpha}$ and q. Relationships between parameters in the expressions for C_m with and without explicit $\dot{\alpha}$-terms can be found in [8]. For partitioned data, the polynomials representing aerodynamic coefficients were postulated without explicit α dependent terms, since the partitioned subspaces span only a 1° range of α.

VI. Flight Data Analysis

The first step in data analysis included a check on data compatibility and the estimation of unknown bias errors in the measurements. Then, from the postulated expressions for aerodynamic coefficients, the structure of these equations was determined and unknown parameters estimated. For the compatibility check, a nonlinear fixed-interval smoother was applied [9]. The fixed-interval smoothing problem can be formulated as follows [9]:

Given a system with state equations

$$x(i+1) = f[x(i), \eta(i)]; \; x(0) = x_0 \tag{2}$$

and measurement equations

$$\begin{aligned} a(i) &= \eta(i) - \xi(i) \\ z(i) &= q\,[x(i)] + n(i) \end{aligned} \tag{3}$$

determine x_0 and the sequence $\xi(i)$, $i=0, 1, \ldots, N-1$ that minimizes the cost function

$$J = \tfrac{1}{2}\{(x_0-\bar{x}_0)^T P_0^{-1}(x_0-\bar{x}_0) + \sum_{i=0}^{N-1}[\xi^T(i)\bar{Q}^{-1}\xi(i) + n^T(i+1)R^{-1}n(i+1)]\} \tag{4}$$

Equation (2) represents the airplane kinematic equations augmented by the equation

$$\dot{\theta} = 0, \; \theta(0) = \theta_0 \tag{5}$$

where the elements of the vector θ are the unknown constant biases and scale factors in the measured data. In eq. (3), $\xi(i)$ is the vector of random errors in measuring the system input $\eta(i)$ and $n(i)$ the vector of random errors in measuring the system output $q[x(i)]$. The input variables are usually represented by angular velocities and linear accelerations or by angular accelerations and derivatives of linear accelerations. When any element of $a(i)$ is unavailable, the corresponding element of $\xi(i)$ is considered to be an unknown forcing function. In eq. (4), $\bar{x}_0$ is an a priori estimate of the state at the initial time, and P_0, Q, and R are the inverse of the weighting matrices. In eqns. (2) to (4), N is the number of data points.

An example of measured and reconstructed (estimated) airspeed and incidence angles is given in Figure 3. In this maneuver, only constant biases and initial conditions were estimated. Because of the very good agreement between the measurements and predictions, it was not necessary to estimate the scale factors. The estimated bias errors in measured data and their standard errors are summarized in Table 1.

All of the corrected data from available maneuvers were analyzed by using a stepwise regression. As a modified version of the linear regression, this method can determine the structure of aerodynamic model equations and estimate the model parameters. The determination of an adequate model for the aerodynamic coefficients includes three steps: the postulation of terms which might enter the model, the selection of an adequate model, and the verification of the model selected. As mentioned in the previous section, the several forms of aerodynamic model equations can be written as

$$y(t) = \theta_0 + \theta_1 x_1(t) + \ldots + \theta_n x_n(t) \tag{6}$$

where $y(t)$ represents the resultant coefficient of the aerodynamic force or moment, θ_1 to θ_n are the stability and control derivatives, θ_0 is the value of any particular coefficient corresponding to the initial conditions, and x_1 to x_n are the HIRM response and control variables or their combinations (see section V). The stepwise regression is a model-building algorithm using the least squares method. All significant terms among the candidate variables are determined and the corresponding parameters are estimated. The variable chosen for entry into the regression equation is the one which has the largest correlation with y after adjusting for the effect on y of the variables already selected. The parameters are estimated by minimizing the cost function

$$J = \sum_{i=1}^{N}\left[y(i) - \theta_0 - \sum_{j=1}^{\ell}\theta_j x_j(i)\right]^2$$

where $\ell+1$ is the number of parameters in the regression equation.

At every step of the regression, the variables incorporated into the model in previous states and a new variable entering the model are reexamined. Any variable which provides a statistically nonsignificant contribution is removed from the model. The process of selecting and checking variables continues until no more variables are admitted into the equation and no more are rejected. The details of the whole procedure are explained in [3] and [8].

VIII. Results and Discussion

Because of the experiment design and type of HIRM's motion, the main emphasis in the flight data analysis was constrained to the lateral aerodynamic equations and the corresponding parameters in these equations. Some of the important lateral parameters are presented to show their variation with α and δ_c and closeness to the wind-tunnel test results. Three maneuvers in flight HD1 and one in HD3 consisted mostly of lightly-damped

large amplitude oscillations, e.g., see Figure 1. The remaining three maneuvers in HD3 flight exhibited large excursions in α with some lateral coupling. The stepwise regression procedure demonstrated that for the oscillatory maneuvers, analyzed as partitioned data, models with linear parameters were adequate for all three lateral coefficients C_Y, C_ℓ, C_n. From the analysis of the individual maneuvers, the technique also selected nonlinear terms $\beta\alpha$ and $p\alpha$ into the model equations for the coefficients C_n. The aerodynamic derivatives C_{Y_β}, C_{ℓ_β}, and C_{n_β} were always selected by the technique as the first parameters for the model equations. They also explain the substantial part of variations in measured data. High sensitivity of the experimental data to these derivatives sometimes resulted in identifiability problems for the remaining parameters (e.g., lower accuracy of their estimates, nonsignificant contribution to the measured responses, etc.).

The estimated values of three static parameters C_{Y_β}, C_{ℓ_β}, and C_{n_β} from data of flights HD1 and HD3 are presented in Figure 4. The parameter values of C_{Y_β} from flight HD3 are not available because of a malfunction of the lateral accelerometer. From the plot of C_{Y_β} against α it is evident that the flight data are consistent except for $\alpha < 23°$ where the flight data are lower than those from the wind tunnel measurements. No explanation for this disagreement was found. The estimates of C_{ℓ_β} from each flight show certain inconsistency for $\alpha < 25°$, but on the average they agree well with the wind-tunnel data. Finally, the flight estimates of C_{n_β} are consistent between flights and agree with the wind tunnel data in trend but show more directional instability of HIRM than predicted by the wind tunnel measurements. As in the case of C_{Y_β}, no reason for this disagreement was found.

In Figure 5, the damping derivative C_{ℓ_p} and cross-derivative C_{n_p} are compared with the results from the oscillatory and rotary wind tunnel tests. The rotary data predicted a decrease in damping for $20° < \alpha < 28°$; whereas, the oscillatory tests show no deterioration in this region. The flight data indicate even less damping-in-roll than the rotary test. The flight results are in agreement with the observed responses of the drop model, which show very little damping or no damping at all. The reason for the discrepancy between the oscillatory data and flight results can be due to the different amplitude of oscillations in the wind tunnel ($\pm5°$) and in flight (around $\pm35°$). The comparison of C_{n_p} parameters from various tests shows a similar pattern to that of C_{ℓ_p}. No nonzero estimates of C_{n_p} could be obtained from the partitioned data for $19° < \alpha < 23°$.

The effect of different canard settings is shown in two examples where $\delta_c = 0°$ and $\delta_h = -18°$. In the upper part of Figure 6, the parameter estimates of C_{ℓ_β} from flights HD2, HD4, and HD6 are plotted and compared with wind-tunnel data for $\delta_h = -20°$ and $\delta_h = -10°$. The consistency of flight estimates is good, and they agree with the wind tunnel data for $\alpha < 32°$. For higher α, the flight results still exhibit negative values for C_{ℓ_β}, but the wind tunnel measurements predict zero and positive dihedral effect. To confirm these differences more flight data would be needed for $\alpha > 32°$. The lower part of Figure 6 contains the damping parameters C_{ℓ_p} from flight and wind-tunnel testing. The rotary test results agree with flight data for $22° < \alpha < 27°$. For the α-region between 27° to 35° the flight data still indicate low damping in roll, which is not confirmed by wind-tunnel measurements. A comparison of flight results in Figure 5 and Figure 6 indicates strong effect of canard setting on damping in roll.

Some of the single maneuvers and partitioned data sets were also analyzed in order to obtain the estimates of longitudinal aerodynamic parameters. The results for the coefficients of the longitudinal and vertical forces were very limited and inconsistent due to insufficient excitation of the airspeed and heave motion. More consistent results were obtained, however, for the pitching-moment parameters. Both the individual maneuvers and partitioned data provided good estimates for the damping and control derivatives and also indicate effects of yawing and rolling velocities on C_m. Figure 7 presents the estimates of C_{m_q} derivative from flights HD1 and HD3. The discrepancy in these results could be caused by different flight conditions and the amplitudes of pitching velocity. The low-amplitude results agree well with wind-tunnel measurements. The second set of flight results shows an increased damping in pitch.

The final set of flight-derived aerodynamic parameters was obtained by averaging and fairing the various estimates for each configuration tested. The first step in the verification of these parameters was the already mentioned comparison with wind-tunnel results. The next step in the verification was made by checking the prediction capabilities of the model equations. This test included the simulation of maneuvers in terms of response variable time histories and time histories of the aerodynamic force and moment coefficients. In Figure 8, the computed and measured time histories of lateral variables from one maneuver in flight HD1 are given. Only three-degree-of-freedom simulation was used, with the longitudinal variables computed from measured data. Figure 8 is completed by the measured time history of the angle of attack, which indicates the α-variation in the measured and simulated data. In Figure 9, the measured and predicted time histories of lateral aerodynamic coefficients from the same maneuver are compared. From both figures it is apparent that the current model can predict the motion of the HIRM within the α-range of 18° to 30° reasonably well. Some deficiencies of the model, however, still remain. The change in the frequency around $\alpha = 23°$ is not accurately predicted, and the amplitudes of computed variables are, in general, greater than those measured. For further improvement of the mathematical model, the analysis of additional flight data would be necessary.

VIII. Concluding Remarks

A procedure for the estimation of an airplane model structure and parameters has been applied to data from a high-incidence research model operating within the α-range of 18 to 40 degrees. The aerodynamic parameters were estimated from individual maneuvers and from subsets of joined data from several maneuvers. The following conclusions can be drawn from the results reported herein:

(1) Because of the nature of HIRM's motion, the

main emphasis in the flight data analysis was concentrated on the lateral parameters. The stepwise regression demonstrated the predominant effect of sideslip parameters on the motion of HIRM. The high sensitivity of experimental data to these parameters sometimes resulted in identifiability problems for the remaining parameters.

(2) The data analysis showed that a linear aerodynamic model was adequate for partitioned data. For individual maneuvers, nonlinear terms expressing the variation of the yawing-moment parameters C_{n_β} and C_{n_p} with the angle of attack were found significant.

(3) The estimated parameters agreed, in general, with the results of wind tunnel measurements. Some differences were, however, observed. The flight data indicated higher directional instability than predicted from the wind tunnel. Within the α-range of 20 to 28 degrees, the estimated oscillatory-roll-rate parameters (damping-in-roll derivative and yawing-moment cross-derivative) exhibited a similar trend as those from wind tunnel rotary test. The flight results, however, showed less damping in roll, which was in agreement with the observed responses of the drop model. The flight results differed significantly from wind tunnel oscillatory test data, which indicated high damping in roll and no variations with the angle of attack.

(4) The current mathematical model based on flight results could predict the motion of the HIRM reasonably well. For the improvement of the model prediction capabilities the analysis of additional flight data would be necessary.

IX. References

1. Moss, G. F.; Ross, A. Jean and Butler, G. F.: A Programme of Work on the Flight Dynamics of Departure Using a High Incidence Research Model (HIRM). RAE Unpublished report, July 1982.

2. Ross, A. Jean and Edwards, Geraldine F.: Correlation of Predicted and Free-Flight Responses Near Departure Conditions of a High Incidence Research Model. Paper 31 of AGARD CP 386, May 1985.

3. Klein, Vladislav and Batterson, James G.: Determination of Airplane Model Structure From Flight Data Using Splines and Stepwise Regression. NASA TP-2126, 1983.

4. Ross, A. Jean and Reid, G. E. A.: The Development of Mathematical Models for a High Incidence Research Model (HIRM) Part 1. Analysis of Static Aerodynamic Data. RAE Techn. Report 83037, 1983.

5. Ross, A. Jean and Reid, G. E. A.: The Development of Mathematical Models for a High Incidence Research Model (HIRM) Part 2. Analysis of Dynamic Test Data. RAE Techn. Report 84072, 1984.

6. Allen, R. J. and Booker, D.: Large-Scale Rolling Rig Tests on the RAE Model 2130 (HIRM 2) in the BAe Warton 5.5m Low-Speed Wind Tunnel. BAe Report AXR103, 1982.

7. O'Leary, C. O.: Dynamic Tests on a High Incidence Research Model (HIRM) in a Low-Speed Wind Tunnel. RAE Techn. Report 84111, 1984.

8. Klein, Vladislav; Batterson, James G. and Murphy, Patrick C.: Determination of Airplane Model Structure From Flight Data Using Modified Stepwise Regression. NASA TP-1916, 1981.

9. Bach, Ralph E., Jr.: A Variational Technique for Smoothing Flight-Test and Accident Data. AIAA Paper 80-1601, 1980.

Acknowledgement

The completion of the research was made possible through the participation and assistance of many people. The authors wish to express their sincere gratitude and appreciation to Dr. A. J. Ross and Mrs. G. F. Edwards from RAE Farnborough, Mr. J. G. Batterson from NASA Langley Research Center and Mr. E. M. Queen from George Washington University.

TABLE 1 - Estimates of bias errors in measured data

MEASURED VARIABLE	BIAS	STANDARD ERROR
V, m/sec	1.6	.63
β, deg	-3.4	.25
α, deg	-1.2	.42
ϕ, deg	-6.	1.1
θ, deg	-1.6	.96
a_x, g units	.04	.020
a_y, g units	.06	.031
a_z, g units	-.12	.015
p, deg/sec	-4.	1.8
q, deg/sec	1.5	.23
r, deg/sec	-3.0	.41

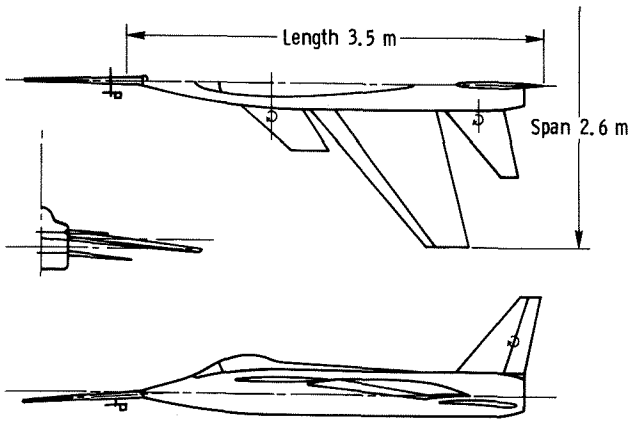

FIGURE 1 - Three-view drawing of test model.

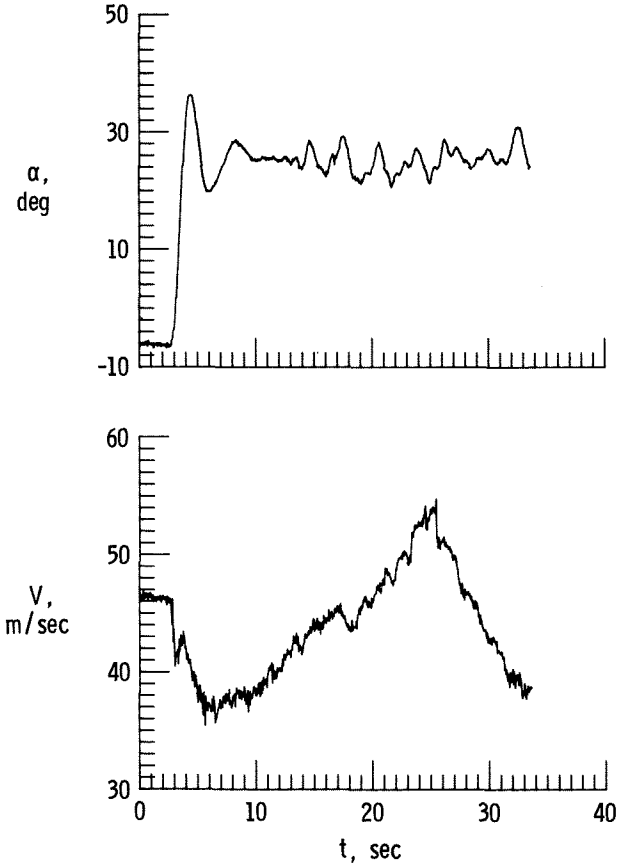

FIGURE 2 - Time histories of measured response variables in a maneuver following the model release from helicopter.

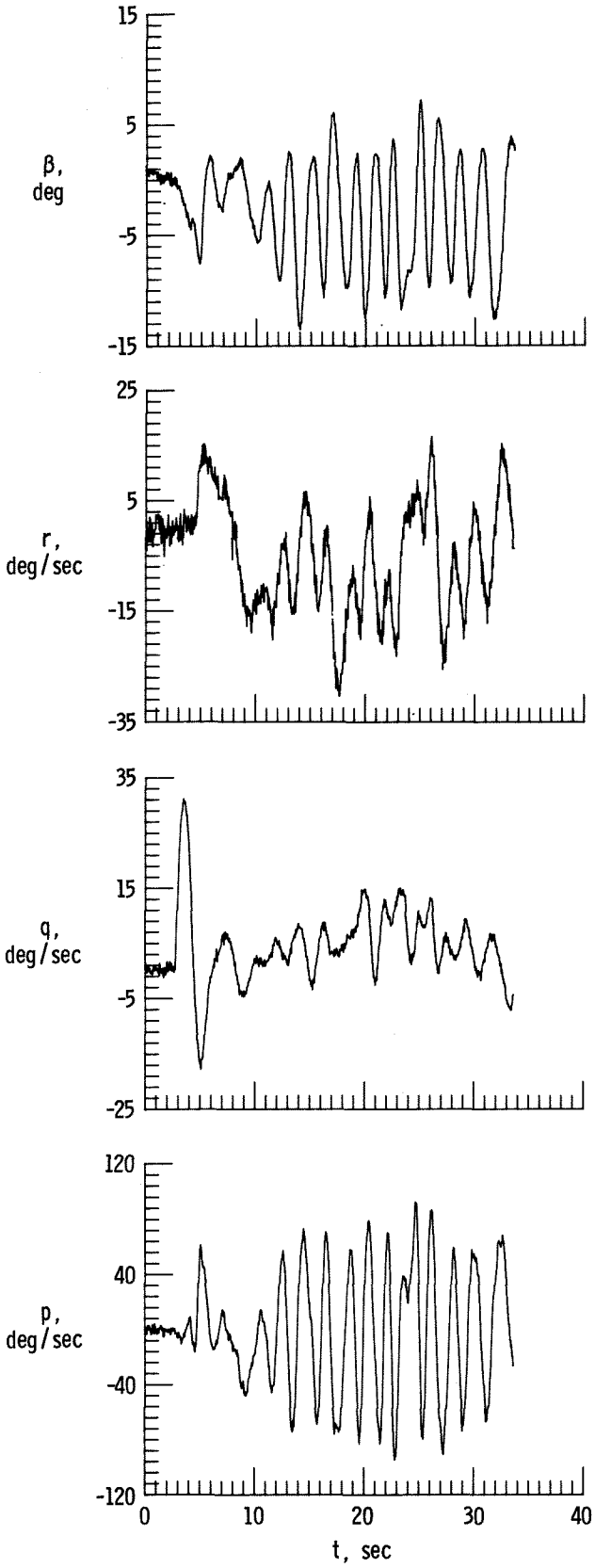

FIGURE 2 - Concluded.

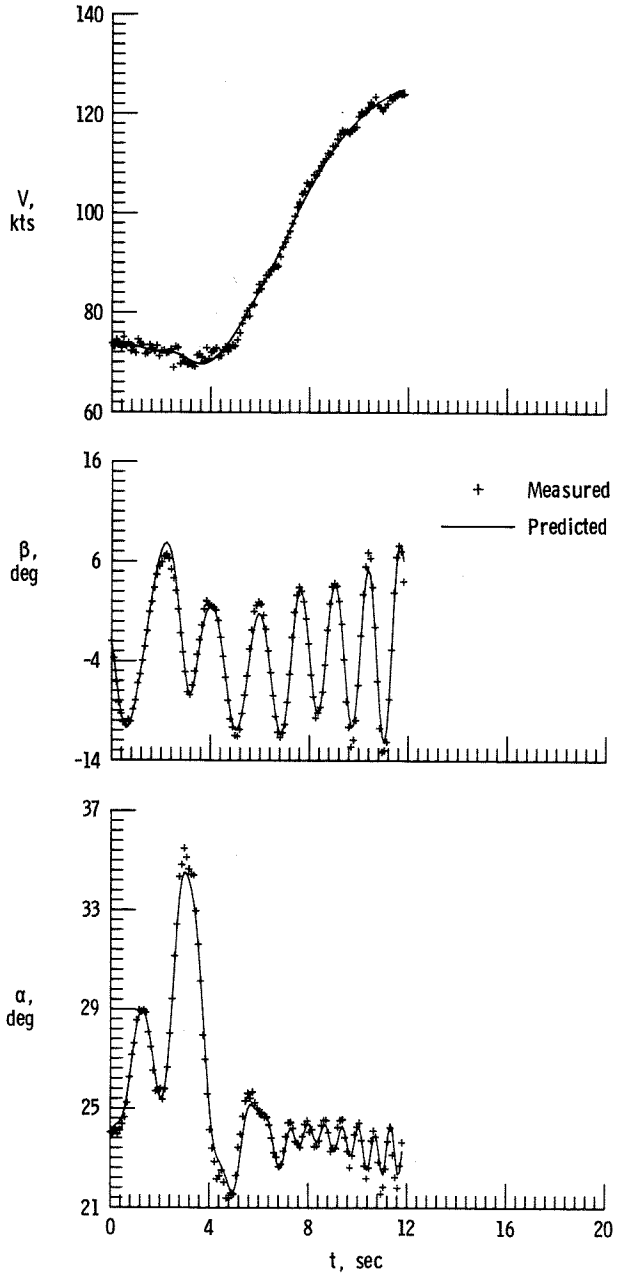

FIGURE 3 - Comparison of measured and predicted time histories in data compatibility check.

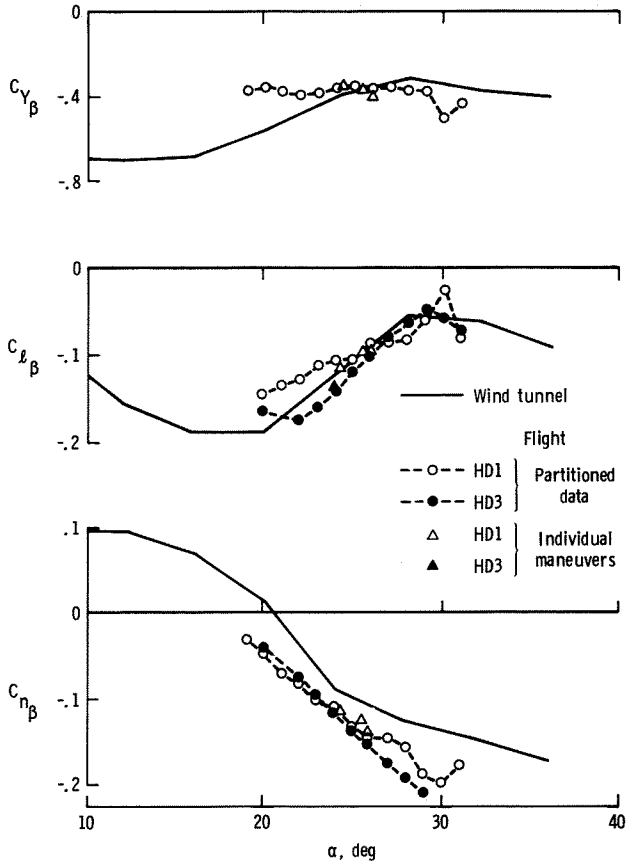

FIGURE 4 - Comparison of parameters expressing sideslip effect estimated from flight data and wind-tunnel measurement.

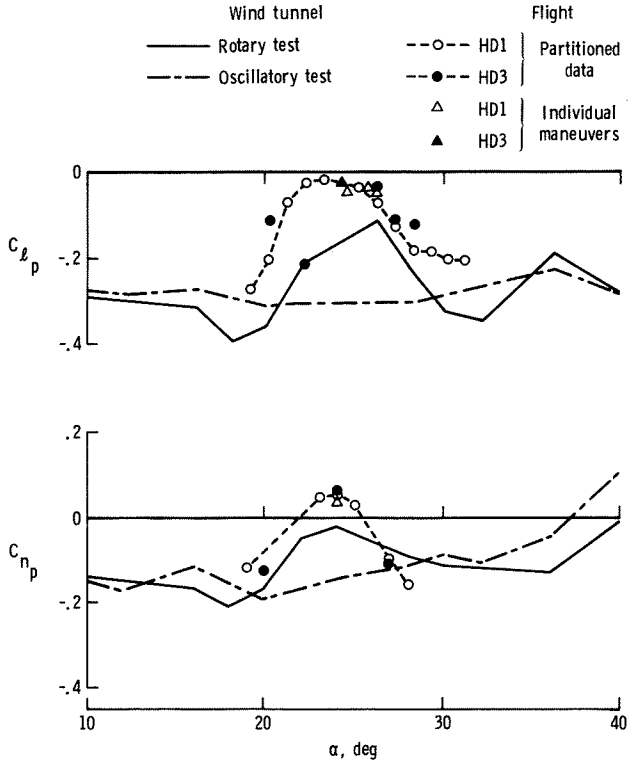

FIGURE 5 - Comparison of oscillatory roll-rate parameters estimated from flight data and wind-tunnel measurement.

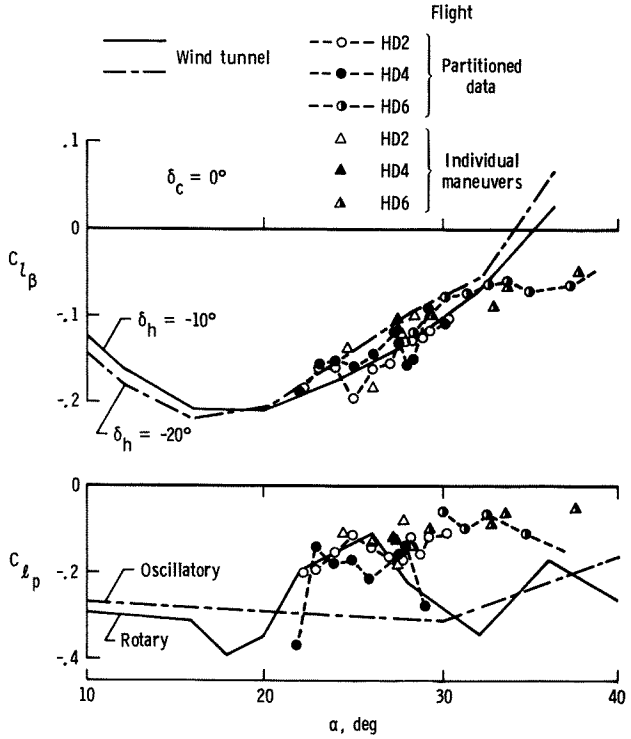

FIGURE 6 - Comparison of sideslip and oscillatory roll-rate parameters estimated from flight data and wind-tunnel measurement.

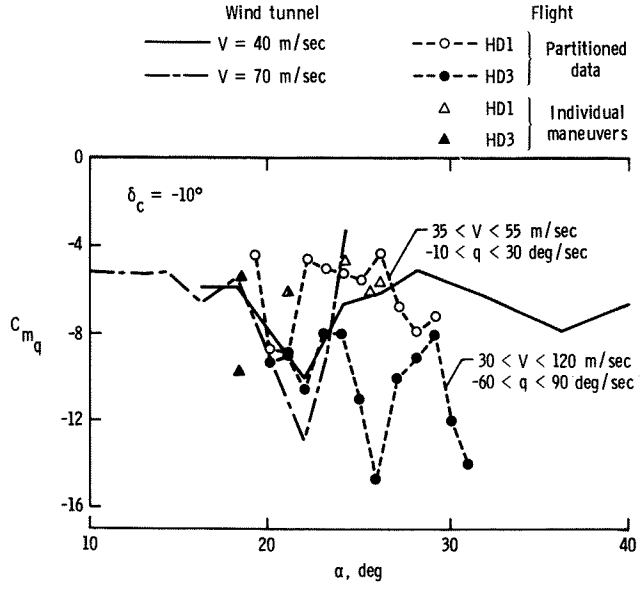

FIGURE 7 - Comparison of damping-in-pitch parameter estimated from flight data and wind-tunnel measurement.

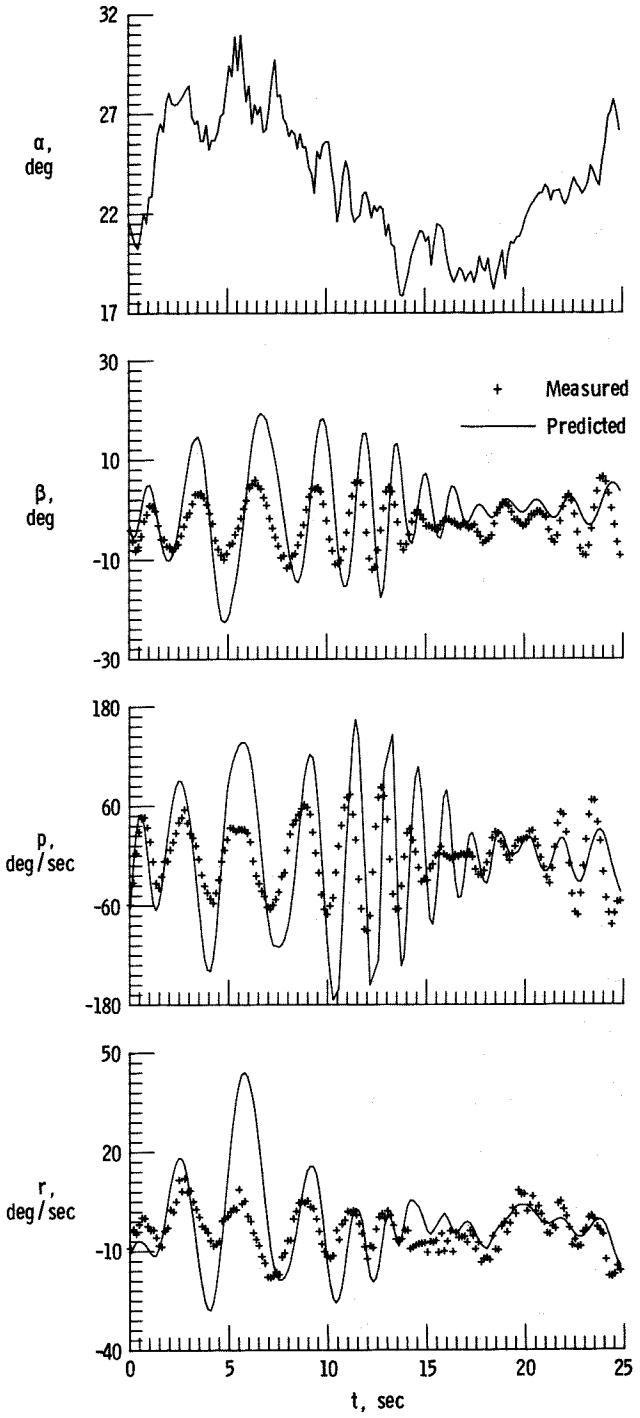

FIGURE 8 - Comparison of measured lateral time histories with those computed from mathematical model of HIRM.

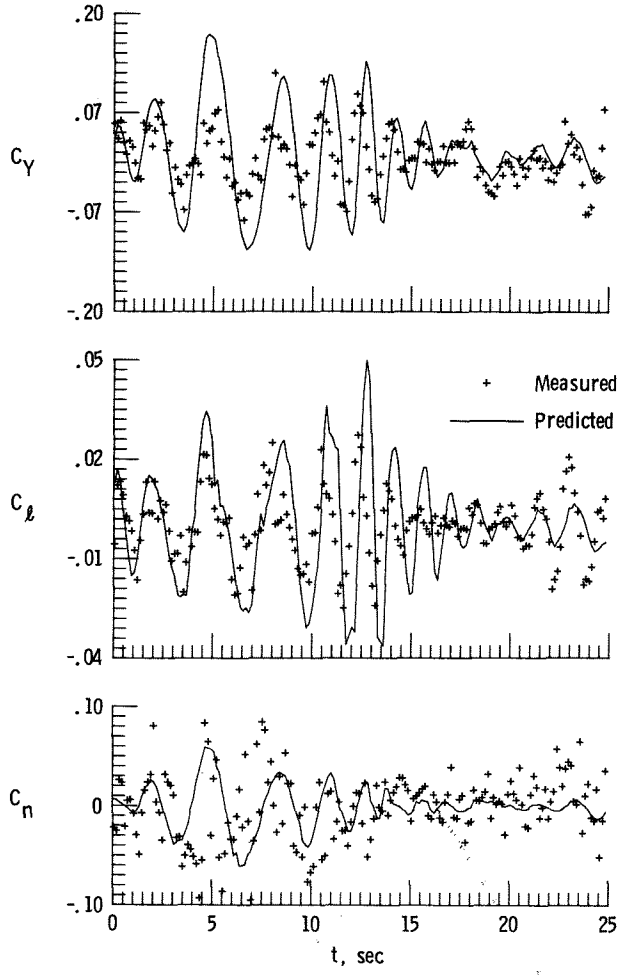

FIGURE 9 - Comparison of measured lateral aerodynamic coefficients with those computed from mathematical model of HIRM.